Hindawi Publishing Corporation
Journal of Chemistry
Volume 2015, Article ID 757256, 13 pages
http://dx.doi.org/10.1155/2015/757256

Research Article

Sorption Characteristics of Mixed Molecules of Glutaraldehyde from Water on Mesoporous Acid-Amine Modified Low-Cost Activated Carbon: Mechanism, Isotherm, and Kinetics

Mukosha Lloyd,[1] Onyango S. Maurice,[1] Ochieng Aoyi,[2] and Taile Y. Leswifi[1]

[1]*Chemical, Metallurgical and Material Engineering Department, Tshwane University of Technology, Private Bag X680, Pretoria 0001, South Africa*
[2]*Chemical Engineering Department, Vaal University of Technology, Andries Potgieter Boulevard, Vanderbijlpark 1900, South Africa*

Correspondence should be addressed to Mukosha Lloyd; loimwimba@yahoo.com

Received 2 September 2014; Revised 7 November 2014; Accepted 1 December 2014

Academic Editor: Claudio Di Iaconi

The environmental discharge of inefficiently treated waste solutions of the strong biocide glutaraldehyde (GA) from hospitals has potential toxic impact on aquatic organisms. The adsorption characteristics of mixed polarized monomeric and polymeric molecules of GA from water on mesoporous acid-amine modified low-cost activated carbon (AC) were investigated. It was found that the adsorption strongly depended on pH and surface chemistry. In acidic pH, the adsorption mechanism was elaborated to involve chemical sorption of mainly hydroxyl GA monomeric molecules on acidic surface groups, while in alkaline pH, the adsorption was elaborated to involve both chemical and physical sorption of GA polymeric forms having mixed functional groups (aldehyde, carboxyl, and hydroxyl) on acidic and amine surface groups. The optimum pH of adsorption was about 12 with significant contribution by cooperative adsorption, elucidated in terms of hydrogen bonding and aldol condensation. Freundlich and Dubinin-Radushkevich models were fitted to isotherm data. The adsorption kinetics was dependent on initial concentration and temperature and described by the Elovich model. The adsorption was endothermic, while the intraparticle diffusion model suggested significant contribution by film diffusion. The developed low-cost AC could be used to supplement the GA alkaline deactivation process for efficient removal of residual GA aquatic toxicity.

1. Introduction

Glutaraldehyde (GA), a five-carbon saturated dialdehyde of two terminal aldehyde groups, is a strong biocide widely used for controlling the growth of microorganisms in hospitals and industries such as paper and pulp with potential environmental release and toxic impact on aquatic organisms [1–4]. Also, GA is widely used as a crosslinking agent in enzyme immobilization technology [5]. Leung [4] found that GA could be stable to abiotic degradation with hydrolysis half-lives of 508, 102, and 46 days in acidic, neutral, and basic aqueous media, respectively. This researcher reported a cyclic dimer of GA to be among major GA degradates in basic aqueous solution, in agreement with reported possible GA self-polymerization products in water [5]. Studies have also revealed acute and chronic toxic impact of GA on aquatic organisms (e.g., algae and fish) [1, 4, 6] and, therefore, GA's potential to disrupt aquatic food web. Of serious concern to environmental pollution are large quantities of concentrated (up to 15000 mg/L) waste GA solutions from cold sterilization of heat sensitive reusable instruments in hospitals that are drained into municipal sewers without safety precautions [2, 3].

The obsolete concept of pollution control by dilution is still relied upon in indiscriminate disposal of hospital toxic wastewaters into municipal sewers. Municipal treatment plants employ the biological treatment which could be limited due to toxicity inhibitory effect and residual toxic pollutants are discharged to receiving water bodies. Pollution control at source point is effective, because dilution does not reduce the absolute number of toxic pollutants entering water

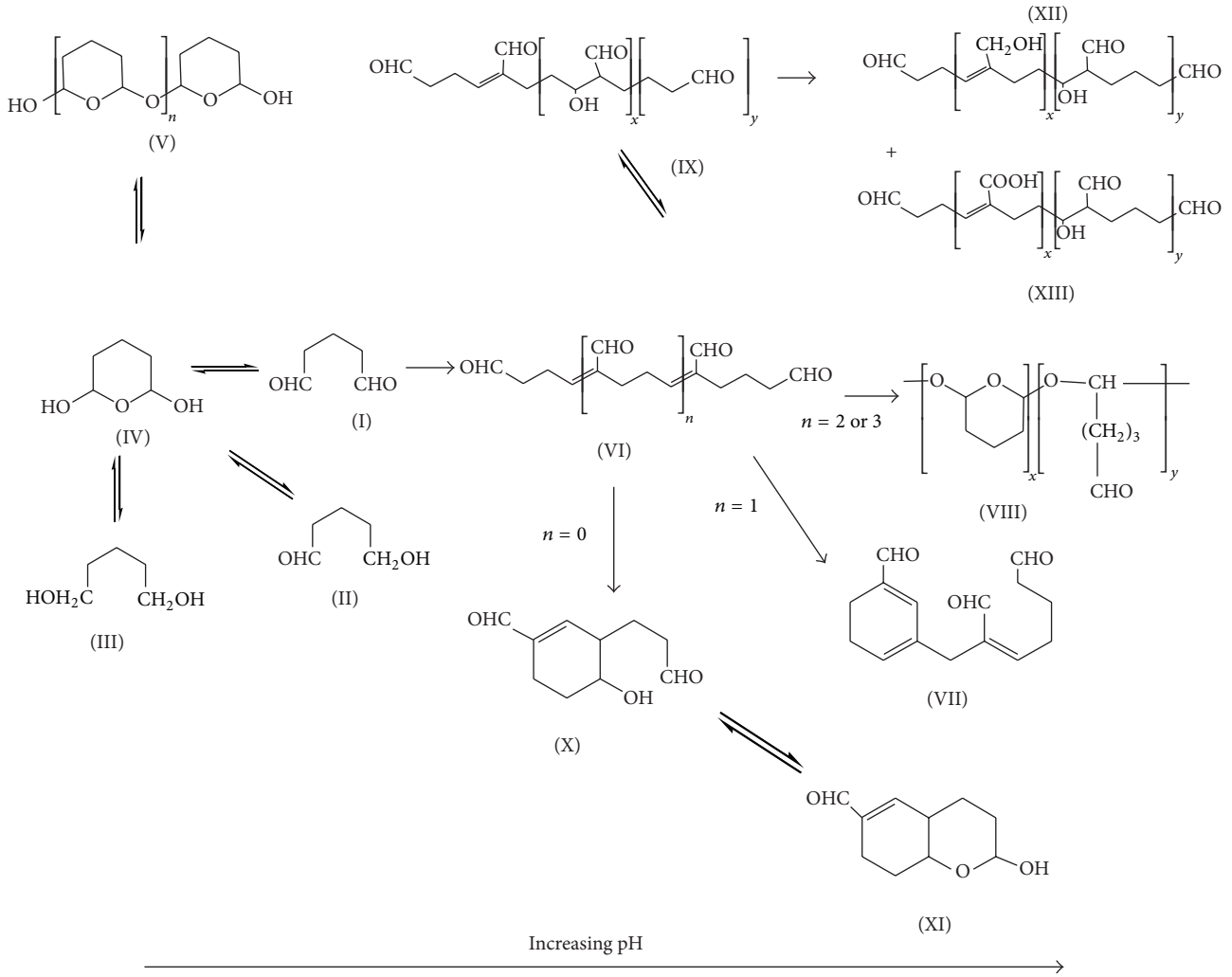

Figure 1: Possible molecular structures of intra-intermolecular polymerization of glutaraldehyde in aqueous solutions. Structure (I): normal glutaraldehyde monomer [5].

bodies and could spell serious hazard in drought periods [2, 7]. An estimate for a worst case scenario for a large urban city like Melbourne, Australia, indicated that concentrated waste GA solution from hospitals could be diluted to 50 mg/L at the sewage treatment plant [3]. GA concentration above 5 mg/L has been reported to be inhibitory for microbial metabolism [4].

The recommended precautionary measure is alkaline deactivation of waste GA solutions before discharge to biological treatment units [3, 4]. However, residual GA aquatic toxicity after chemical deactivation was reported [4]. The two terminal aldehyde groups of GA allow for unique chemistry of pH dependent inter-intramolecular polymerization in water. In alkaline pH, GA undergoes significant polymerization producing reactive/polarized molecules having varied concentrations of aldehyde, hydroxyl, and carboxyl functionalities as shown in Figure 1 [5]. Therefore, supplementary or alternative economical technology(s) for efficient removal of GA from hospital wastewater should be considered.

The activated carbon (AC) adsorption has been rated as the benchmark technology for efficient removal of dissolved organic chemical from water [8]. Whilst GA crosslinking properties in modification of adsorbent [9] and/or immobilization of enzymes [10] have been extensively studied, there is scarce literature on adsorption characteristics of aqueous mixed GA molecules for efficient abatement of the toxic GA from wastewater for environmental protection. Other studies have reported efficient adsorptive removal of monoaldehydes, mostly formaldehyde from water. Tanada et al. [11] modified commercial AC with amino groups for efficient removal of formaldehyde from hospital wastewater. They postulated the adsorption to follow monolayer adsorption. Formaldehyde monolayer adsorption on kaolin and bentonite was also reported [12]. Babić et al. [13] studied the adsorption of pentanal and benzaldehyde on amine modified resin and developed a kinetic model for removal of aldehydes from water. However, GA exists as mixture of polarized monomeric and polymeric molecules as shown in Figure 1. Therefore, it would be expected that GA adsorption characteristics would be different from monoaldehydes.

It is to be noted that the high cost of commercial ACs and/or resins would limit their large scale application in

Table 1: Properties of pine tree (*Pinus patula*) sawdust.

Proximate analysis (wt % db)			Ultimate analysis (wt %)				
Ash	Volatile matter	Fixed Carbon[a]	C	H	S	N	O[a]
0.1	85	15	51	6	0.1	b/d	43

[a]By difference; db: dry basis; b/d: below limit of detection.

wastewater treatment, especially in developing countries [14]. Also, expensive adsorbents would require additional costly regeneration to maximize their value, and this may be difficult to justify in wastewaters treatment for environmental protection [15]. For this reason economical and efficient low-cost adsorbents that can be used on a once-through basis for wastewater treatment are always being sought. We recently developed low-cost AC from South African sawdust using the economical steam activation [16]. We are motivated to explore economical options of value addition to largely wasted South African sawdust for efficient remediation of water pollution.

In this study, our previously developed low-cost AC was acid-amine modified and used to investigate the adsorption characteristics of GA from water. Knowledge of adsorption characteristics of GA would be important for assessing the potential application of low-cost AC for efficient removal of mixed molecules of GA from hospital wastewaters. Due to the nature of mixed polarized GA molecules in water, we considered acid-amine modification of AC and exploit the readily organic solution reactions of aldehyde-amine and/or aldehyde-acid [17] on the AC surface to improve upon GA adsorption. The modified AC was characterized and then tested for batch adsorption of GA from water. The effect of pH was evaluated, and adsorption isotherm and kinetics parameters were determined. A number of possible adsorption interactions are also elaborated.

2. Materials and Methods

2.1. Materials. The parent low-cost AC used was developed from sawdust of Pine tree (*Pinus patula*) obtained locally (Singisi Sawmill, KwaZulu Natal, South Africa). The properties of the *P. patula* sawdust are shown in Table 1. Glutaraldehyde (50 wt.%), 3-methyl-2-benzothiazolinone hydrazone (MBTH), ethylenediamine (EDA, 99%), and toluene were purchased from Sigma, USA. $FeCl_3$, NaOH, NaCl, HNO_3, and HCl were purchased from SMM, South Africa. Deionised water was used for preparation and dilution of chemical solutions. All chemicals used were of analytical grade and were used without further purification.

2.2. Methods

2.2.1. Preparation, Modification, and Characterization of Activated Carbons. A stainless steel vertical fixed-bed tubular reactor heated externally in a controlled temperature electric furnace was used for carbonization and activation of sawdust. Details of preliminary optimization of carbonization/activation processes have been previously reported [16]. Briefly, distilled water washed and overnight oven dried (110°C) sawdust (−4 + 2 mm) was carbonized under N_2 flow (570 mL/min) at 10 K/min from room temperature to 800°C and 2 hrs holding time and cooled to room temperature under N_2 flow. In activation, charred sample(s) was heated at 10 K/min under 180°C preheated N_2 (570 mL/min) to 800°C and activated with superheated steam (180°C, 1.6 bar, and 780 mL/min) for 1.5 hrs, and the AC sample (denoted by A800/1.5) was cooled to room temperature under N_2 flow and stored in a desiccator.

The AC (A800/1.5) was successive chemical modified by carboxylation and amidation [18]. In carboxylation, AC (A800/1.5) was refluxed with 1.5 M HNO_3 in a round bottom flask at a dosage of 1.0 g AC/10 mL HNO_3 for 2 hrs. After HNO_3 refluxing, AC samples (denoted by Nit-AC) were filtered and washed with deionized water to neutral pH and overnight oven dried at 110°C. The amidation of AC (Nit-AC) involved solvent-free refluxing with concentrated EDA solution at a dosage of 1.0 g AC/10 mL EDA for 3 hrs, and AC samples (denoted by EDA-AC) were filtered and washed several times with toluene and overnight oven dried at 110°C and stored in a desiccator.

The textual properties of outgassed AC samples were evaluated at 77 K N_2-adsorption/desorption (Micromeritics 3020). The AC samples surface functionality of aqueous suspension pH was determined by the ASTM D 3838-80 reflux method [19]; pH point of zero charge (pH_{PZC}) by the pH drift method using NaCl background electrolyte with pH (2–12) adjustments by NaOH or HCl solutions additions as detailed in [20]; and total acidity and basicity by neutralization with HCl and NaOH, respectively, following the standardized Boehm titration method [21]. For determination of suspension pH and acidity/basicity triplicate samples were obtained and calculated average and standard deviations reported. Solution pH was measured using the Orion 4 star, pH meter, USA. The bulk density of AC sample was determined using a graduated volumetric cylinder.

The interest in EDA modification of parent AC was to anchor amines groups as sites for condensation of GA molecules through nucleophilic addition reactions [17]. Thus, to check the room temperature stability of amine groups on EDA-AC to changes in pH, we employed a surface groups' stability test of stirring of EDA-AC in 1.5 M HCl solution for 1.0 hr, followed by sequential thorough washing of the AC with NaOH and deionised water to about neutral pH and measuring the resultant aqueous suspension pH of the EDA-AC. A reverse test was also performed using 1.5 M NaOH solution.

2.2.2. Batch Adsorption Equilibrium and Kinetics. In equilibrium adsorption a series of sample bottles with fixed amount of EDA-AC in 25 mL solutions of known glutaraldehyde (GA)

concentrations were placed in a thermostated water shaker at 200 rpm and 24 hrs equilibration. The solutions were then paper filtered and GA concentrations analyzed with UV-Vis spectrophotometer (Schimadzu 620) after derivatization with MBTH reagent and $FeCl_3$ oxidant at 610.5 nm [6]. The adsorption of GA on AC from sample solutions was measured against blank samples (without AC) to factor the possibility of GA abiotic degradation to nonaldehyde products. The effect of pH on GA adsorption and adsorption isotherm parameters at optimum pH of adsorption were evaluated. Triplicate samples were obtained for effect of pH, and average and standard deviations were determined. The pH was adjusted using NaOH or HCl solutions. The equilibrium uptake q_e (mg/g) and percentage uptake Ø (%) were calculated, respectively, as follows:

$$q_e = \frac{(C_o - C_e)V}{m}, \quad (1)$$

$$Ø = 100\left[\frac{(C_o - C_e)}{C_o}\right], \quad (2)$$

where C_o is initial concentration (mg/L), C_e is equilibrium concentration (mg/L), V is solution volume (mL), and m is mass of activated carbon (g).

Batch kinetics was studied at the optimum pH using 600 mL solution of GA in a batch stirred tank. The standard 800 mL capacity laboratory glass beaker was used for the tank and the stirrer was a 45° Pitched four blade impeller of 6 cm diameter, driven by variable speed motor (R50 Ingenieurburo CAT, Germany). In the absence of tank baffles, the stirrer was placed at about 45° angle into the solution to prevent vortex formation and consequential poor mixing of particles and solution. In preliminary experiments the stirrer speed of 400 rpm was observed to impart intense turbulent mixing with complete suspension of particles. A sample of 5 mL aliquot was withdrawn at predetermined time intervals using 0.2 μm syringe filters and analysed for GA concentration with reference to blank samples. The kinetic variables investigated were initial concentration and temperature. The uptake at time t, $q(t)$ (mg/g), was calculated by

$$q(t) = \frac{(C_o - C(t))V}{m}, \quad (3)$$

where $C(t)$ is the concentration of GA (mg/L) in solution at time, t (s).

3. Results and Discussion

3.1. Physical Properties of Activated Carbon Samples. Figure 2 shows the 77 K N_2-adsorption/desorption isotherm curves of parent AC (A800/1.5) and modified ACs (Nit-AC and EDA-AC). The exhibited isotherms were essentially type IV with hysteresis loops due to capillary condensation in mesoporous [22]. However, the nitric acid and amine modifications resulted in successive reductions in N_2 adsorption capacities and proportion of mesopores (reduced size of hysteresis loops). Figure 3 shows the corresponding mesopore pore-size distribution (PSD) determined from desorption curves by

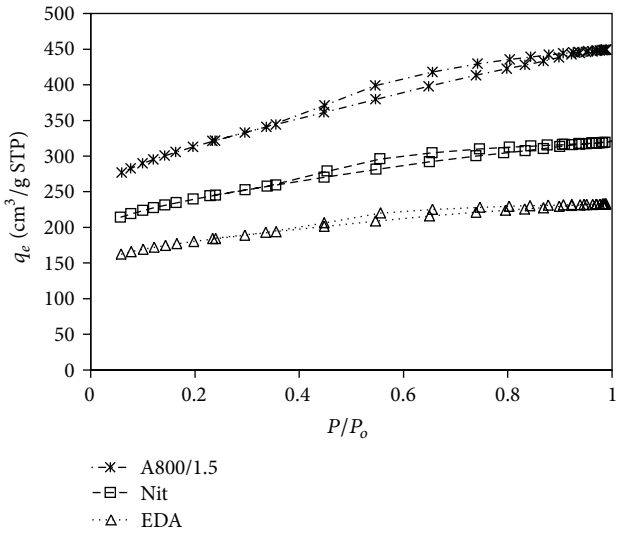

Figure 2: 77 K N_2-adsorption/desorption isotherms of parent AC (A800/1.5) and modified AC samples (Nit-AC and EDA-AC).

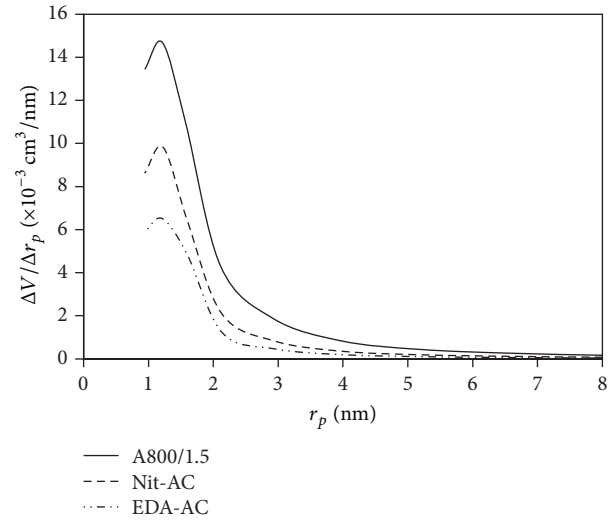

Figure 3: The pore size distribution of activated carbon samples.

the method of Pierce [23], where it was shown that the AC samples had uniform mesoporosity distributions. Apparently, the ACs had the same centre of mesopore PSD at about 2.4 nm pore diameters. However, the AC (A800/1.5) showed a relatively wide uniform mesopore PSD mostly in the range 2.0–8.0 nm pore diameters and with successive modification the intensity and range of mesopore PSD were reduced. Nevertheless, the EDA-AC still maintained narrow uniform mesopore PSD mostly in the range 2.2–5.6 nm pore diameters.

A quantitative summary of the AC samples textural parameters is presented in Table 2. The parent AC (A800/1.5) had high BET surface area (S_{BET}) of 1086 m^2/g and total pore volume (V_T) of 0.69 cm^3/g with high mesopore volume (V_{MESO}) at ca. 62%, therefore providing a suitable porous matrix for grafting acidic and amine groups at reduced

Table 2: Textural properties of activated carbon samples.

AC type	S_{BET} (m^2/g)	S_{MIC} (m^2/g)	V_T (cm^3/g)	V_{MESO} (cm^3/g)	D_{ave} (nm)	ρ_b (g/L)
A800	1086	576	0.69	0.43	2.56	162
Nit-AC	826	489	0.49	0.27	2.39	175
EDA-AC	620	380	0.36	0.19	2.32	230

S_{MIC}: micropore surface area.

Table 3: Surface functionalities of activated carbon samples.

AC type	pH	pH_{PZC}	T_A (μmol/g)	T_B (μmol/g)	N_T (/100 nm^2 AC)
A800/1.5	10.3 ± 0.1	10.3	62.50 ± 1.71	944.44 ± 2.48	55-56
Nit-AC	4.51 ± 0.14	4.00	450.00 ± 2.0	233.33 ± 3.05	49-50
EDA-AC	7.02 ± 0.09	7.10	383.33 ± 3.38	400.00 ± 2.36	75–77

T_A: total acidity; T_B: total basicity; N_A: Avogadro number; N_T: total number of surface groups = $(T_A + T_B)\, N_A/S_{BET}$.

steric hindrance [18]. The results in Table 2 reveal a trend of significant decrease of AC textural parameters with successive chemical modification, consistent with observations in Figures 2 and 3. In the carboxylation stage the loss of S_{BET} and V_{MESO} of the parent AC (A800/1.5) was ca. 24 and 37%, respectively. Following the amidation stage the total loss of S_{BET} and V_{MESO} was ca. 43 and 55%, respectively. Overall, except for BET average pore diameters (D_{ave}) that were similar, the texture properties of EDA-AC were about twice lower than those of AC (A800/1.5). However, the manually measured bulk density (ρ_b) increased in the order AC (A800/1.5) < Nit-AC < EDA-AC, suggesting increased apparent mass of sample due to grafting of acidic and amine surface groups with successive modification. The reduction of textural properties of AC (A800/1.5) in the carboxylation stage can be attributed to the [acid] oxidant selective etching/widening of existing porosity and/or blocking of some pores by grafted acidic surface groups [18, 24, 25]. Further reduction of textural properties in the amidation stage can be attributed to blockage of some pores by grafted EDA molecules [18, 25]. Another contribution to decrease of V_T and V_{MESO} with successive modification would be the introduction of acidic and amine groups in mesopores. However, the EDA-AC still showed a moderate micropore volume ($V_T - V_{MESO}$) of 0.17 cm^3/g and relatively high (V_{MESO}) of 0.19 cm^3/g centred about 2.3 nm pore diameter. A high proportion of mesoporosity (2–50 nm) distribution would be desirable for unconstrained diffusion of large sized GA molecules to interior adsorption wide micropore (0.5–2 nm) which would be sites of high adsorption potential [22, 26]. Otherwise, in aqueous phase application of AC, high proportion of surface narrow microporosity (<0.5 nm) would constrain the diffusion of bulky adsorbate to interior wide micropores through pore blockage.

3.2. Surface Functionalities of Activated Carbon Samples. In aqueous phase adsorption of polarized organic molecules, pore structure and surface chemistry play significant roles [27]. The carboxylation by nitric acid oxidation was included in the AC (A800/1.5) modification scheme so as to increase surface acidic oxygen groups, mainly carboxylic and some phenolic groups [24], on the resultant oxidized AC (Nit-AC). The evolution of surface functionalities of ACs with successive chemical modification is shown in Table 3. The values of pH_{PZC} for AC samples were estimated from Figure 4 at $pH_{initial} = pH_{final}$ [18]. The results in Table 3 indicated that the parent AC (A800/1.5) had alkaline aqueous suspensions pH and pH_{PZC}. This was explained in terms of protonation of large amounts of AC basic surface groups [27]. The in-situ basicity of AC (A800/1.5) could be attributed to decomposition of thermally unstable strong surface acidic oxygen groups that include carboxylic, phenolic, and lactonic groups at the employed high activation temperature of 800°C, leaving a relatively high proportion of thermally stable surface oxygen basic groups postulated to be pyrone-like and chromene [24]. However, it has been argued that the high basicity of high temperature treated AC could mainly be due to Lewis basic sites of the delocalized Π-electrons system on basal graphene layers [20, 24]. Supplementary neutralization tests of the Boehm titration were performed to quantify acidic and basic sites of AC samples [21]. It is known that the selective neutralization cannot quantify all types of surface

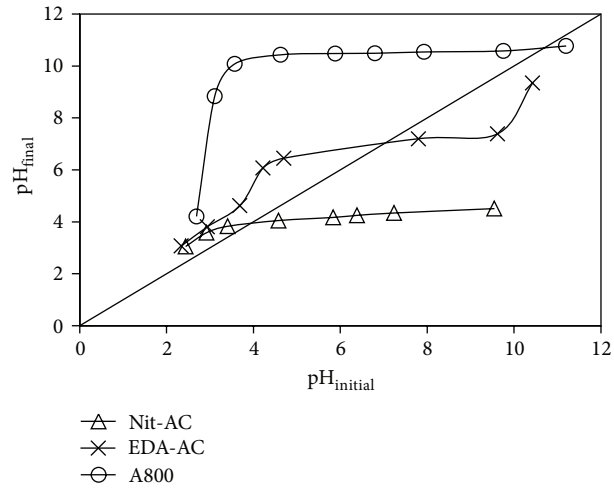

Figure 4: Determination of pH of point of zero charge for activated carbon samples.

acidic and/or basic groups that could be present on AC and, therefore, only total acidity and basicity were measured. From Table 3, the AC (A800/1.5) showed high total basicity (T_B) of about 944.44 μmol/g compared with low total acidity (T_A) of about 62.5 μmol/g, consistent with measured high alkaline aqueous suspensions pH and pH_{PZC}.

It is seen in Table 3 that the nitric acid oxidation shifted the aqueous suspensions pH and pH_{PZC} to acidic range. Acidic suspension pH results from deprotonation of AC acidic surface groups, and this was consistent with measured high acidity of about 450 μmol/g compared with basicity of about 233.33 μmol/g for Nit-AC. The Nit-AC total acidity was about seven times that of AC (A800/1.5), indicative of successful grafting of acidic surface groups on AC (A800/1.5). The employed vigorous HNO_3 refluxing of AC (A800/1.5) would provide stable grafted surface acidic groups through chemical bonding with reactive/unsaturated surface carbon atoms [18, 24].

Following amidation, the aqueous suspensions pH and pH_{PZC} were practically shifted to the neutral range. The acidity of Nit-AC was decreased from about 450 to 383.33 μmol/g, and basicity increased from 233.33 to 400 μmol/g. Since Nit-AC samples were refluxed in pure EDA solution, the increased level of basicity of the EDA-AC sample was indicative of successful grafting of basic amine groups on Nit-AC. The refluxing of EDA with HNO_3 preoxidized AC has been postulated to create stable amine groups through condensation reaction(s) [18]. This is contrasted with surface impregnation of AC which possibly would be unstable surface groups bound by relatively weak physical bonds like electrostatic attraction, ion exchange, and hydrogen bonding. For this case, the physically bind surface groups may be leached from the AC surface with change of pH. In this study, the results of the employed EDA-AC surface groups' stability tests showed that the aqueous suspension pH of EDA-AC remained about neutral, following 1.0 hr stirring in either 1.5 M HCl or NaOH and thorough deionised water washing to neutral pH and overnight 110°C oven drying. This suggested relative stable acidic and amine groups on EDA-AC with variation of pH. It was hypothesized that the EDA refluxing of Nit-AC involved condensation of one amine group of EDA with grafted acidic surface groups through possible amidation reactions as per Figure 5(a) [28] and Figure 5(b), respectively, and that the free amine group of the AC grafted EDA molecule would provide sites for condensation of GA molecules through the readily aqueous nucleophilic addition of amines to aldehydes [17]. It was noted that the measured acidity and basicity of EDA-AC were similar, indicating that not all acidic groups on Nit-AC condensed with EDA molecules consistent with the measured neutral aqueous suspensions pH and pH_{PZC}. Overall, the EDA-AC developed high concentration surface groups (N_T) compared to the other AC samples.

3.3. Effect of pH. The nature of GA monomeric and polymeric molecules in water strongly depends on pH as shown in Figure 1. GA polymerization in water is a consequence of the two terminal aldehyde groups that allow for inter-intramolecular polymerization through aldol condensation reactions

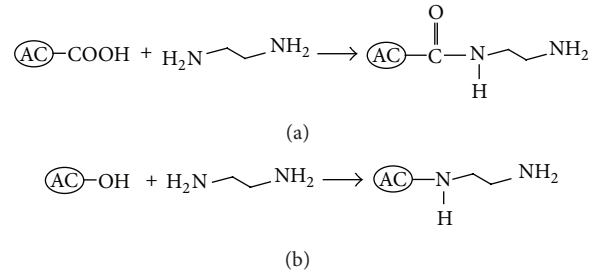

Figure 5

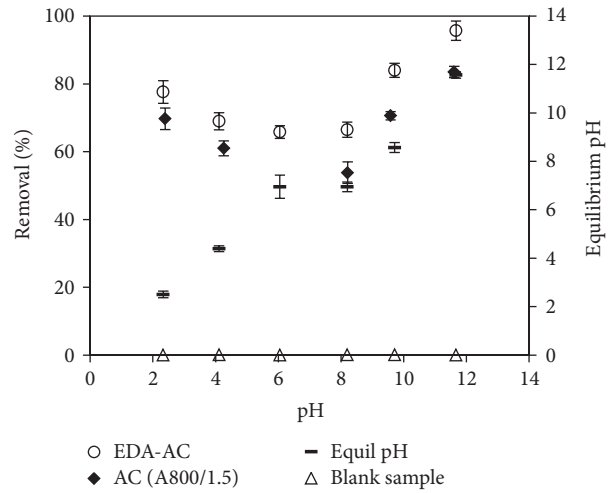

Figure 6: Effect of pH on equilibrium sorption of glutaraldehyde on EDA-AC. C_o: 200 mg/L; 298 K; 0.8 g/L AC; −425 + 150 μm.

catalyzed by solution protons and hydroxyl ions [5]. The evolutions of percentage uptake with pH (2–12) of GA on EDA-AC and parent AC (A800/1.5) as measured against blank samples are compared in Figure 6. Within experimental error, no significant variations in GA or aldehyde concentration of blank samples were measured during 24 hrs experimentation. This was the case for all adsorption tests conducted in this study. In previous study, Leung [4] reported GA thermal stability and hydrolysis degradation half-lives between 508 and 46 days in acidic and basic pH. Essentially, the degradation products of GA in alkaline solution have been found to be polymeric forms of GA having varied concentrations of aldehyde, hydroxyl, and carboxyl functionalities [4, 5]. This means that GA degrades still retain aldehyde properties. Also, GA is soluble in all proportions in water [1, 3], and, at the concentrations (≤450 mg/L) of GA in water used in this study, no GA precipitation was observed in the tested pH (2–12). Therefore, for the proposed treatment/removal of GA from water, the EDA-AC would play a significant role. The results in Figure 6 revealed existence of minima in removal of GA on EDA-AC with an increase in pH, while no significant variation or degradation of GA was measured in blank samples and, therefore, represented at zero percentage removal in Figure 6. For EDA-AC added samples, the removal initially decreased from ca. 78–66% with increase in pH (2–6) and then increased in pH > 8 reaching ca. 96% removal

at pH 11.67. On the other hand, the equilibrium pH slightly increased in pH ≤ 4 and slightly decreased in pH ≥ 8. The same trend for percentage removal was observed on parent AC (A800/1.5). However, the percentage removal at each pH tested was lower on AC (A800/1.5) than on EDA-AC. At pH about 12, there was ca. 13% adsorption enhancement on EDA-AC compared with AC (A800/1.5), and this was considered significant to warrant chemical modification of AC (A800/1.5). As earlier discussed, while both ACs are mesoporous with similar average pore diameters, the textural parameters of AC (A800/1.5) were about twice higher than those of EDA-AC (Table 2). Therefore, we concluded that the adsorption of GA was strongly influenced by AC surface chemistry, in this case increased postactivation reflux condensed surface acidic and amine groups on EDA-AC.

Since the adsorption of GA was strongly dependent on pH and surface acidic and amine groups, we proposed several surface adsorption interactions as follows. For pH < 7, the EDA-AC surface is net positively charged ($pH_{PZC} \approx 7.2$) due to protonation of surface native basic groups, grafted amine groups (pKa = 7.46), and phenolic hydroxyls (pKa = 9.63) [29], consistent with slightly raised equilibrium pH. On the one hand, a large fraction of carboxylic surface groups would be deprotonated (pKa = 2.08) [29]. In the solution phase GA monomers of hydroxyl functionality are predominant, Figure 1. Therefore, it was postulated that, for pH < 7, specific adsorption interactions could occur through complexation involving covalent bonding of carboxyl-hydroxyl condensation as per Figure 7(a). The low adsorption of GA on AC (A800/1.5) was attributed to reduced acidic surface groups compared with EDA-AC (Table 3). For pH > 7, the EDA-AC surface assumed net negative charge due to deprotonation of surface basic and acidic groups, consistent with slightly reduced equilibrium pH. In the solution phase GA polymers having mixed aldehyde, hydroxyl, and carboxyl functionalities are predominant, Figure 1. Therefore, for pH > 7 it was postulated that specific adsorption interactions could occur through covalent bonding reactions such as carboxyl-hydroxyl Figure 7(b); carboxyl-aldehyde Figure 7(c); hydroxyl-aldehyde Figure 7(d); and amine-aldehyde (formation of Schiff bases) Figure 7(e). Also, physical electrostatic attraction could occur through amine-hydroxyl Figure 7(f) and amine-carboxyl Figure 7(g). Consequently, the high adsorption of GA on EDA-AC compared with AC (A800) in pH > 7 could be attributed to grafted amino and [high] acidic surface groups on the former AC. Further insight into the adsorption mechanism was gained from the study of adsorption isotherm.

3.4. Adsorption Isotherm. Figure 8 shows the equilibrium isotherm for sorption of GA on EDA-AC. In the experimental C_o (150–450 mg/L), the isotherm curve was suggestive of type III or type V isotherms typical of multilayer or cooperative adsorption [30]. The type V isotherm was more likely the case because EDA-AC had a relatively high mesopore volume fraction (Table 2). In principle, the existence of different polarized GA molecules having at least common aldehyde functionality(s) in solution would entail competition for same adsorption sites. However, the prediction of mixed GA molecules adsorption equilibrium data using multicomponent adsorption models (e.g., the real ideal adsorption solution theory [31]) could be exceedingly difficult due to mutual causes of significant nonideality introduced by cooperative adsorption and different types and unknown amounts of individual components present at any pH, and GA monomeric and polymeric molecules in water are in equilibrium [5] and, therefore, it is difficult to isolate and experimentally determine monocomponent isotherm parameters. Thus, to determine isotherm parameters relevant to optimal design of adsorption units for sorption of GA on EDA-AC, the classical isotherm models of Freundlich and Dubinin-Radushkevich (D-R) were fitted to the experimental multilayer isotherm data. The Freundlich isotherm is one of the empirical models that can be applied to multilayer adsorption on heterogeneous surfaces and is defined by [32]

$$q_e = K_F \left(C_e\right)^{\mathrm{Fr}}, \tag{4}$$

where K_F is the Freundlich adsorption constant (mg/g) and Fr is the heterogeneity factor.

The D-R isotherm model was originally formulated from the Polanyi adsorption potential and used to effectively describe adsorption of gases and vapours on microporous adsorbents at high and intermediate solute concentrations [33]. The D-R model is usually used to give an idea about the type of adsorption [33, 34]. Over the past years, however, the D-R model has been extended to describe adsorption from aqueous phase [26, 34]. Applied to liquid phase adsorption the D-R isotherm is defined by

$$\begin{aligned} q_e &= Q_{\max} \exp\left(-B_D \epsilon^2\right), \\ \epsilon &= RT \ln\left(1 + \frac{1}{C_e}\right). \end{aligned} \tag{5}$$

The characteristic of the D-R isotherm is given by

$$\varphi = \frac{1}{\sqrt{2B_D}}, \tag{6}$$

where $Q_{\max}$ is the maximum adsorption capacity (mg/g), B_D is the activity coefficient related to the mean sorption energy (mol^2/kJ^2), ϵ is the Polanyi adsorption potential (kJ/mol), and φ is the mean sorption energy (kJ/mol). The magnitude of φ provides information on the type of adsorption: the range $8 < \varphi < 16$ kJ/mol indicates chemical adsorption, whereas $\varphi <$ 8 kJ/mol indicates physical adsorption.

The Freundlich and D-R isotherm models were fitted to isotherm data by nonlinear regression of minimizing the Chi-square (χ^2) between experimental and model uptakes (7) [32]. The solutions to the Chi-squared test were generated using Microsoft Excel 2007, Add-in solver, and results presented in Table 4. Consider

$$\chi^2 = \sum_{j=1}^{n} \frac{\left(q_{e(\mathrm{expt})_j} - q_{e(\mathrm{calc})_j}\right)^2}{q_{e(\mathrm{expt})_j}}. \tag{7}$$

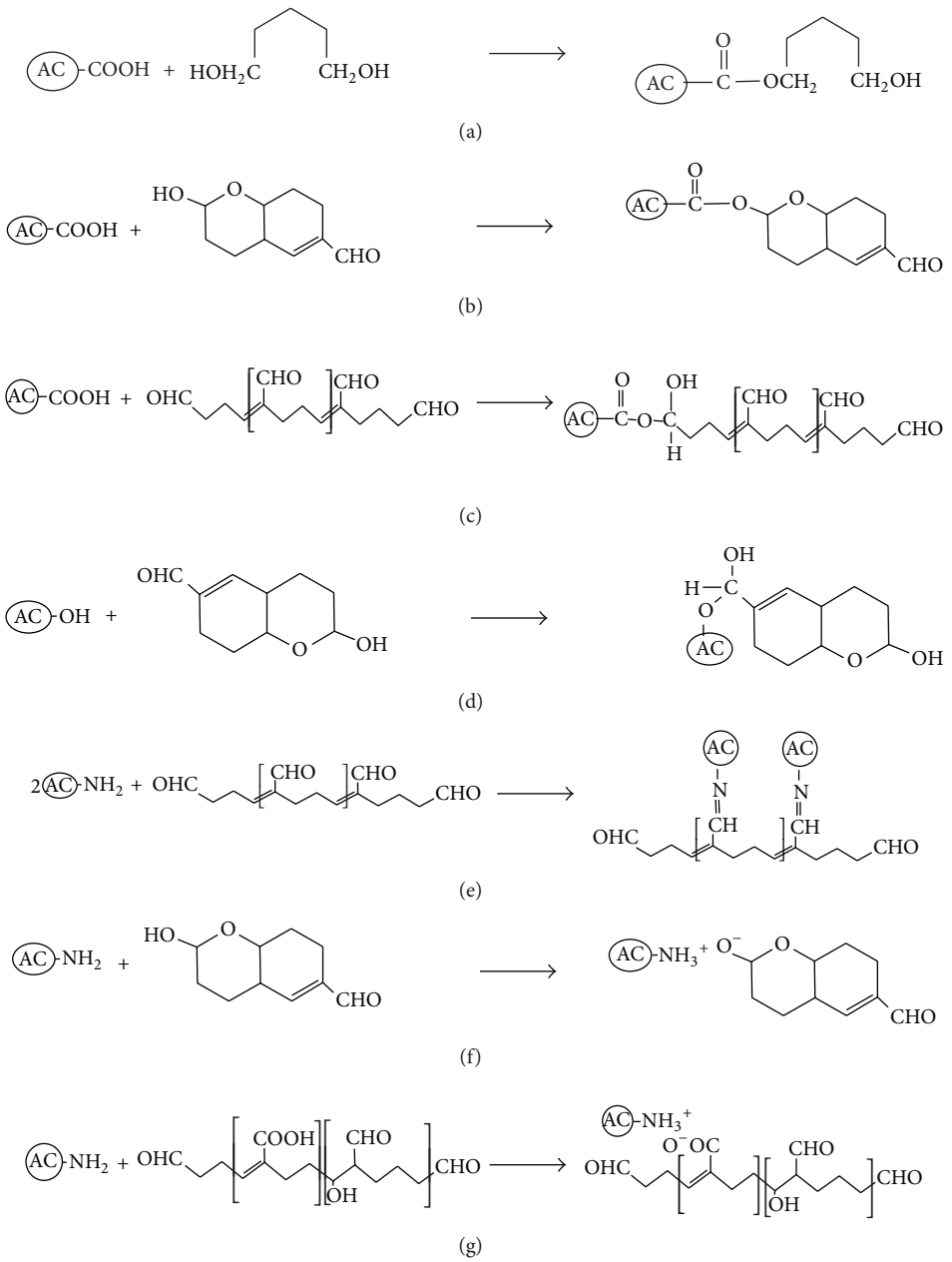

Figure 7

Table 4: Isotherm parameters for sorption of glutaraldehyde on EDA-AC.

Freundlich constants			D-R constants			
K_F (mg/g)	Fr	χ^2	Q_{max} (mg/g)	B_D (mol^2/kJ^2)	φ (kJ/mol)	χ^2
5.36	1.34	2.24	431.04	25.40	0.14	6.67

The results in Table 4 indicated that the Freundlich model well described the isotherm data. The Freundlich heterogeneity factor, Fr > 1, was confirmation of multilayer adsorption of GA on EDA-AC [32]. However, the exponential nature of the Freundlich model implies infinite amount of adsorption which was not the case because some residual GA always remained in solution after 24 hrs equilibration. Although not being the best fit compared to the Freundlich model based on the Chi-squared (χ^2) test, the D-R model also closely approximated the equilibrium data as observed in Figure 8. The D-R model has theoretical basis in thermodynamics principles [33] and was used to estimate the equilibrium adsorption capacity and the apparent mean sorption energy of GA on EDA-AC. The D-R estimated adsorption capacity (Q_{max}) was 431 mg/g and the apparent mean sorption energy (φ) was 0.47 kJ/mol. The magnitude of $\varphi < 8$ kJ/mol suggested

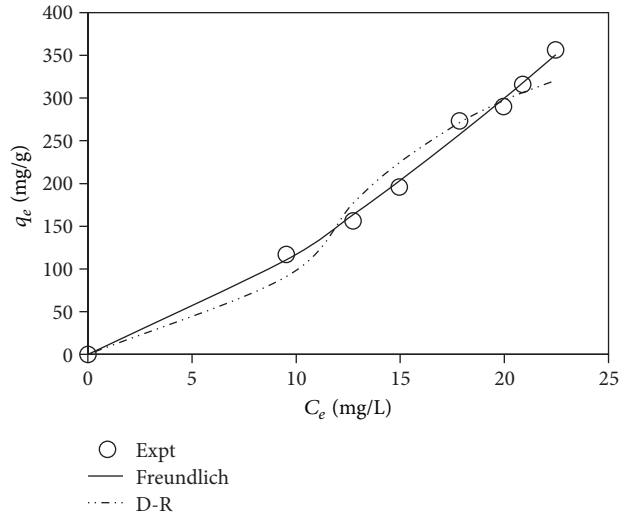

Figure 8: Adsorption isotherm for sorption of glutaraldehyde on EDA-AC: 298 K; 0.8 g/L AC; pH 11.6 ± 0.2; −425 + 150 μm.

that the binding of GA on EDA-AC may be dominated by physical adsorption [34].

A feature of cooperative adsorption is interaction energies among polarized functional groups in adsorbed and solution molecules [30]. For example, the increased adsorption of water vapour on degassed or more hydrophobic charcoal has been attributed to cooperative adsorption through hydrogen bonding [35]. In the case of adsorption of polar GA molecules on the polar heterogeneous EDA-AC surface of distributed adsorption potential, specific adsorbent-adsorbate interactions of the types proposed in Figures 7(a)–7(g) would be more favourable in wide micropores of high adsorption potential [36]. On the other hand, intermolecular hydrogen bonding among hydroxyl, carboxyl, and aldehyde groups of adsorbed and solution GA monomers and/or polymers would be more favourable in mesopores of relatively weak adsorption potential. The aldehyde groups function only as hydrogen bond acceptors. This may be the reason why multilayer adsorption through hydrogen bonding for formaldehyde adsorption on amine modified AC was not reported in [11]. Another possible contribution to GA cooperative adsorption could be aldol condensation reactions among aldehyde groups of adsorbed and solution monomeric and/or polymeric molecules [17]. The postulated hydrogen bonding and aldol condensation mechanisms for cooperative sorption of GA are depicted in Figure 9. Referring to results in Figure 4, the high adsorption of GA at pH 11.6 can be attributed to predominance of polymers having high concentrations of hydroxyl and aldehyde functionalities (Figure 1) and, therefore, high intermolecular interaction energies of hydrogen bonding and/or aldol condensation.

3.5. Adsorption Kinetics

3.5.1. Effect of Initial Concentration. The adsorption kinetics of GA on EDA-AC is integral to the optimal design of adsorption units for it affects the throughput [37]. The effect of initial concentration, C_o (150 and 200 mg/L), and contact time on batch sorption of GA on EDA-AC is shown in Figure 10. The uptake at both C_o was rapid in the initial adsorption time and gradually decreased for later times. This was attributed to diminishing concentration gradient with increase in contact time. At all contact times the uptake was always higher at 200 mg/L than at 150 mg/L, results attributable to high concentration gradients at high initial concentration. At both C_o, equilibrium time was not reached after 360 minutes, possibly due to the multilayer adsorption nature of GA on EDA-AC. However, in the initial 20 min the percentage removals were ca. 55 and 48% for 150 and 200 mg/L, respectively, indicative of good performance considering the low EDA-AC dosage of 0.8 g/L.

The optimum design of batch GA adsorption units by use of the contact time model suitable for low-cost EDA-AC would require knowledge of the reaction rate constant [37]. To estimate the applicable rate constant for sorption of GA on EDA-AC, the adsorption kinetics reaction models of the pseudosecond order and Elovich were fitted to adsorption kinetics data. The pseudosecond order model is defined by (8) [37], and the Elovich model is defined by (9) [38]. Consider

$$q_t = \frac{q_2 k_2 t}{1 + q_2 k_2 t} = \frac{ht}{q_2 + ht}, \tag{8}$$

$$q_t = \frac{1}{\beta} \ln(\sigma\beta) + \frac{1}{\beta} \ln t, \tag{9}$$

where q_2 is the theoretical pseudosecond order adsorbed quantities (mg/g); k_2 is the pseudosecond order rate constant (g/mg min); h is pseudosecond order initial sorption rate (mg/g min); β is constant characteristic of the process (g/mg) and σ is the initial sorption rate (mg/g min).

The applicability of the kinetics reaction model to kinetics data was validated by lowest nonlinear Chi-squared function (χ^2) calculated from (7). The calculated kinetics parameters are presented in Table 5.

The results in Table 5 indicated that the Elovich kinetics model adequately described the kinetics data as observed in Figure 10. The Elovich kinetics model is formulated on surface chemisorption kinetics [38] and, therefore, its close fit to kinetics data was confirmative of chemisorption contributing to binding of GA on EDA-AC surface. As earlier discussed complexation/condensation reactions would involve covalent bond formation as shown in proposed Figures 7(b)–7(e) and aldol condensation. The analysis of results in Table 5 showed that the constant β increased with an increase in C_o. On the other hand, the initial sorption rate σ decreased with an increase in C_o. Juang and Chen [38] have reported the existence of maxima in σ with an increase in C_o for sorption of metal cations on resin. This can be attributed to diffusional limitations due to increased surface coverage at high C_o.

3.5.2. Effect of Temperature. The effect of temperature and contact time on the batch sorption of GA on EDA-AC is shown in Figure 11. The uptake with time increased with an increase in temperature, which indicated endothermic adsorption, that is, involvement of chemical adsorption. The

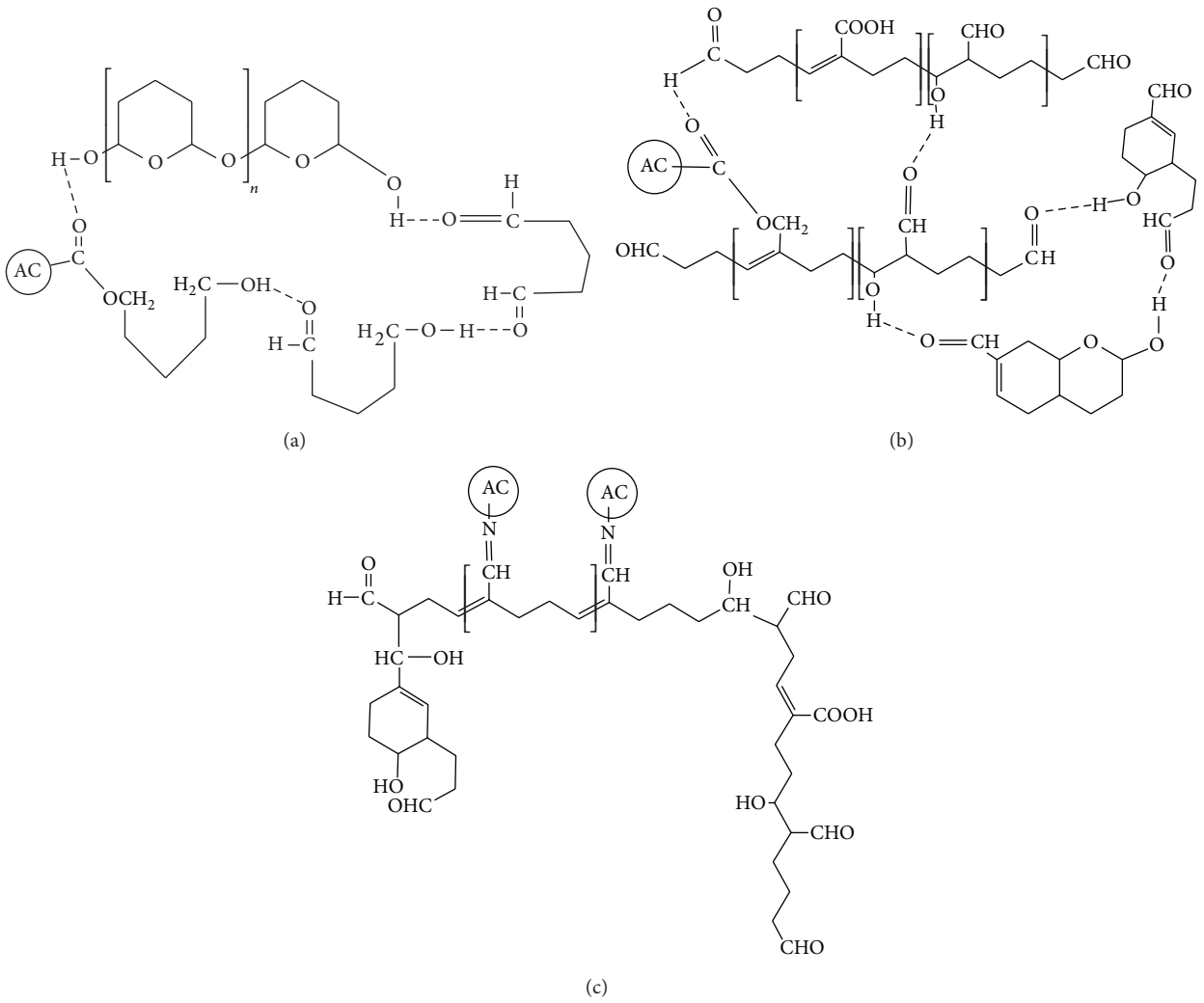

Figure 9: Schematic illustrations of possible glutaraldehyde cooperative adsorption mechanisms: (a) hydrogen bonding, pH < 7; (b) hydrogen bonding, pH > 7; and (c) aldol condensation, strong alkaline pH.

Table 5: Batch kinetics rate constants for sorption of glutaraldehyde on EDA-AC.

Variable	$q_{e(\text{Expt.})}$ (mg/g)	Pseudosecond order				Elovich		
		q_2 (mg/g)	k_2 (g/mg min)	h (mg/g min)	χ^2	β (g/mg)	σ (mg/g min)	χ^2
C_O (mg/L)	(Particle size: −425 + 300 μm; T: 296 K)							
150	170.15	146.77	0.001	22	22	202.42	0.051	4
200	205.85	182.37	0.006	199	20	108.72	0.037	3
Temp. (K)	(C_O: 150 mg/L; particle size: −425 + 300 μm)							
296	170.15	146.77	0.001	22	22	202.42	0.051	4
305	174.53	170.95	0.009	263	6	295.63	0.047	3
314	175.42	177.27	0.001	31	7	495.74	0.048	5

increase of uptake rate with an increase in temperature may be due to increased polymerization rate of GA with an increase in temperature [3]. At temperatures 314 and 305 K the adsorption process seemed to have reached equilibrium after 200 min, whereas equilibrium was not reached after 360 min at 296 K. The parameters for pseudosecond order and Elovich models on effect of temperature as determined by minimizing the Chi-squared test are presented in Table 5. The results in Table 5 indicated that the Elovich model adequately described the kinetics data at all temperatures studied. The β values increased with an increase in temperature. The σ values were similar with an increase in temperature. Since GA polymerization rate in water increases with an increase in temperature [3], it would be expected that the initial sorption

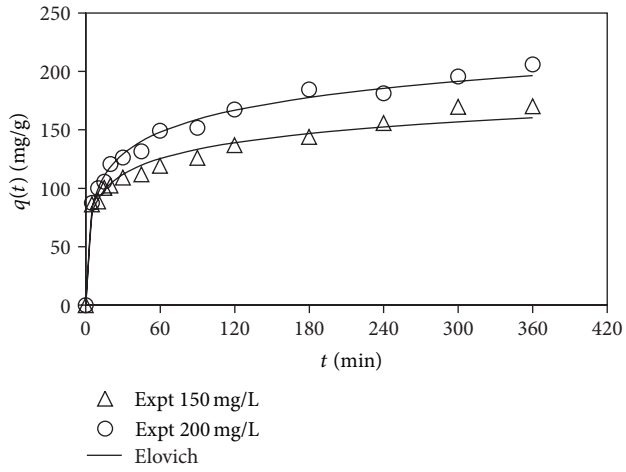

Figure 10: Effect of initial concentration on batch kinetics for sorption of glutaraldehyde on EDA-AC. 296 K; 0.8 g/L AC; pH 11.73 ± 0.03; −425 + 300 μm.

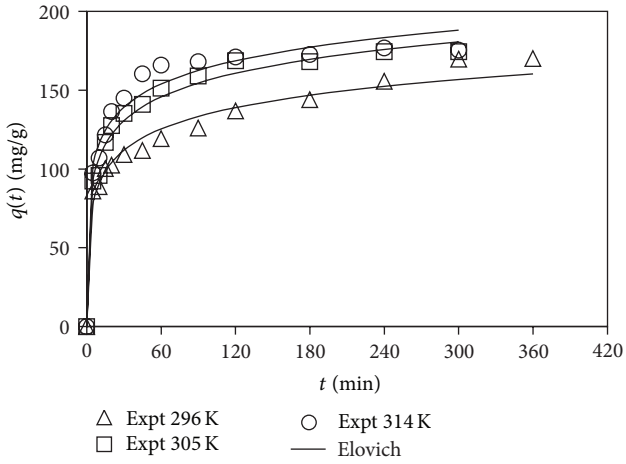

Figure 11: Effect of temperature on batch kinetics for sorption of glutaraldehyde on EDA-AC. C_o: 150 mg/L; 0.8 g/L AC; pH 11.56 ± 0.03; −425 + 300 μm.

rate would increase with increase in temperature. Due to increased size, the polymeric molecules of GA would be relatively less water soluble and, therefore, would preferentially partition to the AC phase rapidly as they are formed. The observed similar values of σ with increase in temperature were suggestive of adsorption diffusional limitations. To elucidate the diffusion mechanism, the kinetics data were further analyzed by the intraparticle diffusion model [39]:

$$q(t) = K_I t^{0.5} + C, \tag{10}$$

where K_I (mg/g h$^{0.5}$) is the intraparticle diffusion rate constant. The linear plot of (10) gives an idea of the adsorption rate-controlling step. The intercept C reflects the resistance to mass transfer in the external or liquid-film. If the plot is linear and passes through the origin, then intraparticle diffusion is the only rate-limiting step.

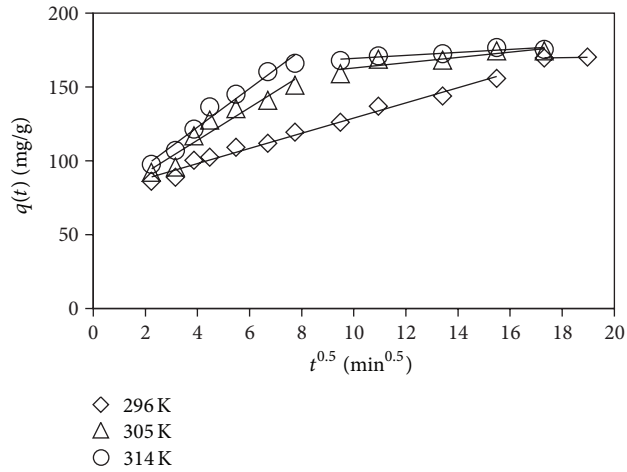

Figure 12: Intraparticle diffusion plots for sorption of glutaraldehyde on EDA-AC.

The linear fitting of the intraparticle model to sorption of GA on EDA-AC at different temperatures is shown in Figure 12. The plots at all temperatures did not pass through the origin, indicative of the intraparticle diffusion not being the only rate-limiting step. The high intercepts were suggestive of strong contribution of the liquid-film mass transfer to the sorption process, especially in the initial adsorption period [39]. As the adsorption progresses, the second limiting transfer stage (initial steep stages in Figure 12) could be the consequence of intraparticle diffusion presumably due to molecules crowding the surface and, therefore, competition for adsorbent pores [40]. The levelled final transfer stages could be described in terms of adsorption equilibrium condition. It was observed that equilibrium was attained earlier at 305 and 315 K than at 296 K, consistent with results in Figure 11.

4. Conclusion

This study provided information on the adsorption characteristics of mixed molecules of glutaraldehyde (GA) on mesoporous acid-amine modified low-cost activated carbon. The information is important for assessing the potential application of activated carbon (AC) adsorption for efficient removal of GA from discharged hospital waste GA solution. The acid-amine modification of the low-cost AC significantly improved the adsorption of GA from water. It was found that the amount of GA adsorbed was strongly dependent on acidic and amine surface groups. Also, there was strong contribution by multilayer adsorptions due to presence of polarized molecules in both the adsorbed and solution phases. The optimum pH of adsorption was about 12 with estimated Dubinin-Radushkevich capacity of 431 mg/g. The results of this study indicated that the developed acid-amine modified low-cost AC could be used for efficient removal of GA from water. By nature of mixed GA molecules in water, acidic surface groups seemed to play a significant role in the overall adsorption process. Thus, this study needs further

investigations to evaluate the adsorption behaviour of GA on oxidized or acid modified low-cost AC.

Conflict of Interests

The authors declare that there is no conflict of interests regarding the publication of this paper.

Acknowledgment

The authors gratefully acknowledge the support of this project by the National Research Fund of the Tshwane University of Technology, Pretoria, South Africa.

References

[1] E. Emmanuel, K. Hanna, C. Bazin, G. Keck, B. Clément, and Y. Perrodin, "Fate of glutaraldehyde in hospital wastewater and combined effects of glutaraldehyde and surfactants on aquatic organisms," *Environment International*, vol. 31, no. 3, pp. 399–406, 2005.

[2] B. Jolibois, M. Guerbet, and S. Vassal, "Glutaraldehyde in hospital wastewater," *Archives of Environmental Contamination and Toxicology*, vol. 42, no. 2, pp. 137–144, 2002.

[3] National Industrial Chemicals Notification and Assessment Scheme (NICNAS), "Priority existing chemicals No.3 Glutaraldehyde," Full Public Report, National Industrial Chemicals Notification and Assessment Scheme (NICNAS), New South Wales, Australia, 1994, http://www.nicnas.gov.au/publications/car/pec/pec3/pec_3_fid.

[4] H.-W. Leung, "Ecotoxicology of glutaraldehyde: review of environmental fate and effects studies," *Ecotoxicology and Environmental Safety*, vol. 49, no. 1, pp. 26–39, 2001.

[5] I. Migneault, C. Dartiguenave, M. J. Bertrand, and K. C. Waldron, "Glutaraldehyde: behavior in aqueous solution, reaction with proteins, and application to enzyme crosslinking," *BioTechniques*, vol. 37, no. 5, pp. 790–802, 2004.

[6] L. L. Sano, A. M. Krueger, and P. F. Landrum, "Chronic toxicity of glutaraldehyde: differential sensitivity of three freshwater organisms," *Aquatic Toxicology*, vol. 71, no. 3, pp. 283–296, 2005.

[7] B. Jolibois, M. Guerbet, and S. Vassal, "Detection of hospital wastewater genotoxicity with the SOS chromotest and ames fluctuation test," *Chemosphere*, vol. 51, no. 6, pp. 539–543, 2003.

[8] R. M. Clark and B. W. Lykins, *Granular Activated Carbon, Design, Operation and Cost*, MI Lewis, Chelsea, Mich, USA, 1989.

[9] S.-I. Park, I. S. Kwak, S. W. Won, and Y.-S. Yun, "Glutaraldehyde-crosslinked chitosan beads for sorptive separation of Au(III) and Pd(II): opening a way to design reduction-coupled selectivity-tunable sorbents for separation of precious metals," *Journal of Hazardous Materials*, vol. 248-249, no. 1, pp. 211–218, 2013.

[10] D. I. Bezbradica, C. Mateo, and J. M. Guisan, "Novel support for enzyme immobilization prepared by chemical activation with cysteine and glutaraldehyde," *Journal of Molecular Catalysis B: Enzymatic*, vol. 102, pp. 218–224, 2014.

[11] S. Tanada, N. Kawasaki, T. Nakamura, M. Araki, and M. Isomura, "Removal of formaldehyde by activated carbons containing amino groups," *Journal of Colloid and Interface Science*, vol. 214, no. 1, pp. 106–108, 1999.

[12] M. Salman, M. Athar, U. Shafique et al., "Removal of formaldehyde from aqueous solution by adsorption on kaolin and bentonite: a comparative study," *Turkish Journal of Engineering and Environmental Sciences*, vol. 36, no. 3, pp. 263–270, 2012.

[13] K. Babić, L. G. J. van der Ham, and A. B. de Haan, "Sorption kinetics for the removal of aldehydes from aqueous streams with extractant impregnated resins," *Adsorption*, vol. 14, no. 2-3, pp. 357–366, 2008.

[14] A. Ahmad, M. Rafatullah, O. Sulaiman, M. H. Ibrahim, Y. Y. Chii, and B. M. Siddique, "Removal of Cu(II) and Pb(II) ions from aqueous solutions by adsorption on sawdust of Meranti wood," *Desalination*, vol. 247, no. 1-3, pp. 636–646, 2009.

[15] M. Streat, J. W. Patrick, and M. J. Camporro Perez, "Sorption of phenol and para-chlorophenol from water using conventional and novel activated carbons," *Water Research*, vol. 29, no. 2, pp. 467–472, 1995.

[16] L. Mukosha, M. S. Onyango, A. Ochieng, and H. Kasaini, "Development of better quality low-cost activated carbon from South African Pine tree (*Pinus patula*) sawdust: characterization and comparative phenol adsorption," *International Journal of Chemical, Nuclear, Metallurgical and Materials Engineering*, vol. 7, no. 7, pp. 228–238, 2013.

[17] J. McMurry, *Organic Chemistry*, Books/Cole, Pacific Grove, Calif, USA, 5th edition, 2000.

[18] A. Houshmand, W. M. A. W. Daud, and M. S. Shafeeyan, "Exploring potential methods for anchoring amine groups on the surface of activated carbon for CO_2 adsorption," *Separation Science and Technology*, vol. 46, no. 7, pp. 1098–1112, 2011.

[19] M. Valix, W. H. Cheung, and G. McKay, "Preparation of activated carbon using low temperature carbonisation and physical activation of high ash raw bagasse for acid dye adsorption," *Chemosphere*, vol. 56, no. 5, pp. 493–501, 2004.

[20] M. V. Lopez-Ramon, F. Stoeckli, C. Moreno-Castilla, and F. Carrasco-Marin, "On the characterization of acidic and basic surface sites on carbons by various techniques," *Carbon*, vol. 37, no. 8, pp. 1215–1221, 1999.

[21] S. L. Goertzen, K. D. Thériault, A. M. Oickle, A. C. Tarasuk, and H. A. Andreas, "Standardization of the Boehm titration. Part I. CO_2 expulsion and endpoint determination," *Carbon*, vol. 48, no. 4, pp. 1252–1261, 2010.

[22] H. Marsh and F. Rodriguez-Reinoso, *Activated Carbon*, Elsevier, Oxford, UK, 1st edition, 2006.

[23] S. J. Gregg and K. S. W. Sing, *Adsorption, Surface Area and Porosity*, Academic Press, London, UK, 1982.

[24] M. F. R. Pereira, S. F. Soares, J. J. M. Órfão, and J. L. Figueiredo, "Adsorption of dyes on activated carbons: influence of surface chemical groups," *Carbon*, vol. 41, no. 4, pp. 811–821, 2003.

[25] H. Tamai, K. Shiraki, T. Shiono, and H. Yasuda, "Surface functionalization of mesoporous and microporous activated carbons by immobilization of diamine," *Journal of Colloid and Interface Science*, vol. 295, no. 1, pp. 299–302, 2006.

[26] C.-T. Hsieh and H. Teng, "Influence of mesopore volume and adsorbate size on adsorption capacities of activated carbons in aqueous solutions," *Carbon*, vol. 38, no. 6, pp. 863–869, 2000.

[27] C. Moreno-Castilla, "Adsorption of organic molecules from aqueous solutions on carbon materials," *Carbon*, vol. 42, no. 1, pp. 83–94, 2004.

[28] Z. Li, X. Chang, X. Zou et al., "Chemically-modified activated carbon with ethylenediamine for selective solid-phase extraction and preconcentration of metal ions," *Analytica Chimica Acta*, vol. 632, no. 2, pp. 272–277, 2009.

[29] E. K. Putra, R. Pranowo, J. Sunarso, N. Indraswati, and S. Ismadji, "Performance of activated carbon and bentonite for

adsorption of amoxicillin from wastewater: mechanisms, isotherms and kinetics," *Water Research*, vol. 43, no. 9, pp. 2419–2430, 2009.

[30] R. C. Bansal and M. Goyal, *Activated Carbon Adsorption*, CRC Press, London, UK, 2005.

[31] A. Erto, A. Lancia, and D. Musmarra, "A Real Adsorbed Solution Theory model for competitive multicomponent liquid adsorption onto granular activated carbon," *Microporous and Mesoporous Materials*, vol. 154, pp. 45–50, 2012.

[32] K. Y. Foo and B. H. Hameed, "Insights into the modeling of adsorption isotherm systems," *Chemical Engineering Journal*, vol. 156, no. 1, pp. 2–10, 2010.

[33] N. D. Hutson and R. T. Yang, "Theoretical basis for the Dubinin-Radushkevitch (D-R) adsorption isotherm equation," *Adsorption*, vol. 3, no. 3, pp. 189–195, 1997.

[34] C. Duran, D. Ozdes, A. Gundogdu, and H. B. Senturk, "Kinetics and isotherm analysis of basic dyes adsorption onto almond shell (Prunus dulcis) as a low cost adsorbent," *Journal of Chemical and Engineering Data*, vol. 56, no. 5, pp. 2136–2147, 2011.

[35] R. C. Bansal, T. L. Dhami, and S. Prakash, "Surface characteristics and surface behaviour of polymer carbons. I. Associated oxygen and hydrogen," in *Activated Carbon Adsorption*, R. C. Bansal and M. Goyal, Eds., pp. 106–107, CRC Press, London, UK, 2005.

[36] Y. El-Sayed and T. J. Bandosz, "Acetaldehyde adsorption on nitrogen-containing activated carbons," *Langmuir*, vol. 18, no. 8, pp. 3213–3218, 2002.

[37] Y. S. Ho and G. McKay, "A two-stage batch sorption optimized design for dye removal to minimize contact time," *Process Safety and Environmental Protection*, vol. 76, no. 4, pp. 313–318, 1998.

[38] R.-S. Juang and M.-L. Chen, "Application of the elovich equation to the kinetics of metal sorption with solvent-impregnated resins," *Industrial & Engineering Chemistry Research*, vol. 36, no. 3, pp. 813–820, 1997.

[39] K. Li, Y. Li, and Z. Zheng, "Kinetics and mechanism studies of p-nitroaniline adsorption on activated carbon fibers prepared from cotton stalk by $NH_4H_2PO_4$ activation and subsequent gasification with steam," *Journal of Hazardous Materials*, vol. 178, no. 1–3, pp. 553–559, 2010.

[40] A. Kumar and S. Kumar, "Adsorption of resorcinol and catechol on granular activated carbon: equilibrium and kinetics," *Carbon*, vol. 41, no. 15, pp. 3015–3025, 2003.